Environmental Science Nano

PAPER

View Article Online
View Journal | View Issue

Cite this: *Environ. Sci.: Nano*, 2019, 6, 2171

Effects of typical engineered nanomaterials on 4-nonylphenol degradation in river sediment: based on bacterial community and function analysis†

Piao Xu,‡[ab] Ming Chen,‡[ab] Cui Lai,‡[ab] Guangming Zeng,*[ab] Danlian Huang,*[ab] Han Wang,[ab] Xiaomin Gong,[ab] Lei Qin,[ab] Yuanyuan Liu,[c] Dan Mo,[ab] Xiaofeng Wen,[ab] Chengyun Zhou[ab] and Rongzhong Wang[ab]

In this study, we presented a detailed investigation on the effects of typical engineered nanomaterials (ENMs) (including Fe_2O_3 nanoparticles, Fe_3O_4 nanoparticles and multi-wall carbon nanotubes (MWCNTs)) on 4-nonylphenol (4NP) degradation based on the diversity and function of bacterial communities in sediments. The results demonstrated that iron oxides promoted 4NP degradation and enzyme activities in sediments, while MWCNTs inhibited these activities. LEfSe analysis suggested that iron oxides incorporation discriminative enriched iron-reducing bacteria including *Pantoea*, *Shewanella* and *Shewanellaceae* contributed to iron reduction and organic degradation. PICRUSt analysis demonstrated that 4NP contamination promoted the expression of genes related to biodegradation, including amino acid metabolism, carbohydrate metabolism, energy metabolism and xenobiotic biodegradation and metabolism. Interestingly, compared to MWCNTs, iron oxide incorporation resulted in enhanced expressions of iron-regulated proteins including ferric uptake regulator (Fur), diphtheria toxin regulator (DtxR), and ferrous iron transport (FeoB) and iron complex transport systems. These results indicate that iron oxides have a better advantage in 4NP degradation; in contrast, the pragmatic evaluation of the prospects of MWCNTs is necessary due to the persistence of 4NP in sediments. This study may be favorable to evaluate secure applications of ENMs in the aquatic environment based on a full understanding of their environmental fate.

Received 1st April 2019,
Accepted 16th May 2019

DOI: 10.1039/c9en00371a

rsc.li/es-nano

Environmental significance

Given the complexity of evaluating the environmental implications of engineered nanomaterials (ENMs) (inevitable co-occurrence of chemical contaminants and microbes) in natural sediments, understanding their interactions is challenging. This study investigates the impacts of ENMs on 4-nonylphenol (4NP) degradation based on the diversity and function of bacterial communities. Most importantly, iron-reducing bacteria, iron-regulated proteins and iron cycles in sediment bacteria were innovatively investigated, considering their vital roles in 4NP degradation. The study may be favorable to evaluate the secure applications of ENMs in the aquatic environment based on a full understanding of their environmental fate.

1. Introduction

The increase in the global production and application of engineered nanomaterials (ENMs) has resulted in their increasing release into the environment. A recent study estimated that approximately 20 000 t of ENMs are expected to end up in municipal incineration facilities worldwide on an annual basis.[1] Among numerous ENMs, iron-based and carbon-based nanomaterials are widely applied and discharged. CNTs have been proposed for large-scale applications, such as hydrogen storage devices, quantum computers, agricultural smart delivery systems, chemical sensors, optical devices, catalyst supports, and also environmental applications.[2] Numerous

[a] *College of Environmental Science and Engineering, Hunan University, Changsha 410082, P.R. China. E-mail: zgming@hnu.edu.cn, huangdanlian@hnu.edu.cn; Fax: +86 731 88823701; Tel: +86 73 88823701*
[b] *Key Laboratory of Environmental Biology and Pollution Control, Ministry of Education, Hunan University, Changsha 410082, P.R. China*
[c] *College of Chemistry and Chemical Engineering, Changsha University of Science and Technology, Changsha 410076, P.R. China*

† Electronic supplementary information (ESI) available: Additional information about ENM properties and bacterial community and function analysis are provided in the supporting information. Content includes Fig. S1–S4 and Table S1. See DOI: 10.1039/c9en00371a

‡ These authors contribute equally to this article.

studies have demonstrated the wide applications of iron oxide nanomaterials (*e.g.*, Fe_2O_3, Fe_3O_4 and FeOOH) in ceramics, leather, catalysts and wastewater treatment.[3,4] According to a market research report, the production capacity for carbon nanotube (CNT) products was about 4065 tons in 2010 and exceeded to 12 300 tons in 2015.[5] The significant expansion in the applications of these ENMs in large-scale commercial applications led to their eventual accumulation in the environment. Once released into the environment, ENMs may accumulate in soils and/or sediments.

As the ultimate sink of various pollutants, aquatic sediments tend to be the primary storage for ENMs as well. There is a growing concern about the fate of ENMs and their interactions with co-existing contaminants due to their potential effects on transformation and bioavailability.[6,7] Additionally, once accumulated in the soils/sediments, ENMs may contact with soil particles, contaminants, and microorganisms. Microorganisms, as a vital component in the ecosystem, play an important role in the fate of contaminants and ENMs. The published data on the fate of ENMs in the environment have primarily focused on their effect on the transportation and bioavailability of contaminants usually in a simulated porous medium or soil. For example, Hofmann and von der Kammer[8] investigated the synergetic transport between carbon nanomaterials and hydrophobic organic pollutants (HOCs) in porous media and proved that carbon nanomaterials can act as pollutant carriers to influence the transport of pollutants.

Specifically, 4-nonylphenol (4NP) has drawn increasing concern due to its estrogenic effects and ubiquity in the environment.[9,10] For example, the production and consumption loads of 4NP in the United States were reported to be 194 000 tons and 163 000 tons, respectively, in 2006.[11] Meanwhile, 4NP is a breakdown product of nonylphenol ethoxylates (NPEs) widely used in detergents, textiles and pesticides,[12] but it is more persistent, lipophilic and toxic than the parent NPEs.[13] Approximately 60% of NP is released into the aquatic environment *via* the discharge of wastewater treatment plant (WWTP) effluents mainly as the intermediate product of NPEs.[14] Commonly, 4NP can be potentially removed by the naturally occurring microorganisms present in sediments, and bacterial strains with bioremediation potentials have also been identified. Several bacterial strains isolated from soils, sediments or activated sludge were found to participate in the direct degradation of 4NP, and these include *Pseudomonas* sp.,[15] *Sphingomonas* sp.[16,17] and *Stenotrophomonas* sp.[18] Drastic shifts in microbial activity and bacterial community members largely driven by organic contaminants have been widely reported in pure soil or river sediment.[19,20] Previous studies demonstrated that such contaminations stimulated the enrichment of organic-degrading microbial community.[21,22] Exploring microbial communities can provide invaluable information on the biological understanding of biodegradation. However, only few studies have concentrated on investigating the microbial response to the co-existence of ENMs and organic contaminants, which is beneficial for controlling the risks of ENMs based on the understanding of their interactions. In particular, very few studies have been done on natural sediments because of the uncertainty and complexity of their dynamic characteristics.

To address the lack of information about the interactions between NPEs and ENMs, especially how bacterial community and functions are affected by and respond to the stress associated with the co-existence of organic pollutants and ENMs, this study aims to explore the interactions among ENMs, environmental contaminants, and bacterial communities and their implications on the microbial functions in sediments. Accordingly, the actual environmental risks posed by ENMs are mainly determined by the species and bioavailability of ENMs in the environment. Numerous studies have demonstrated the application of iron oxide nanomaterials (*e.g.*, Fe_2O_3, Fe_3O_4 and FeOOH) and multi-wall carbon nanotubes (MWCNTs) to remove contaminants or lower the bioavailability in wastewater.[2–4] Hence, we chose Fe_3O_4 nanoparticles, Fe_2O_3 nanoparticles and MWCNTs, which are widely applied and discharged,[23–25] as representative ENMs. Typically, our study combines distinctive bacterial function analysis based on PICRUSt to provide a more complete investigation of the sediment microbiological state than that typically reported. In this study, we aimed to (1) evaluate the effect of typical ENMs on 4NP transformation and degradation in the water–sediment interface, (2) determine the bacterial community response in sediments driven by 4NP contamination and ENM incorporation, and (3) explore the variation of bacterial metabolism functions in these perturbed sediments to elucidate the impacting mechanisms associated with each ENM.

2. Materials and methods

2.1. Materials

Sediment samples were collected from the 5–15 cm layer from the surface in the Xiangjiang River along the Xiaoxiang road near the Hunan University in Changsha, China. After air drying, sediments were ground and passed through a 2 mm sieve prior to the experiments. The sediments had a neutral pH (6.76) and an organic carbon content of 24.9 g kg^{-1}. Fe_2O_3 nanoparticles and Fe_3O_4 nanoparticles (>99.5% purity) were purchased from Jingkang New Material Technology Co. Ltd (Changsha). MWCNTs (>98% purity) were purchased from Chengdu Organic Chemicals Co. Ltd. of the Chinese Academy of Sciences. Detailed information, including shape, size and surface areas of MWCNTs and iron oxide nanoparticles, is provided in Table S1 (ESI†). Ultrapure water was used throughout the experiments.

2.2. Experiment setup

Natural sediment with ultrapure water was set as blank control (group A). Natural sediment with 4NP supernatant was also used as a control setup (group B). ENM-incorporated sediment was prepared by adding Fe_3O_4 nanoparticles (group

C), Fe_2O_3 nanoparticles (group D) or MWCNTs (group E) at a mass proportion of 0.5%. The prepared ENM–sediment mixtures were then homogenized *via* agitation at 30 rpm for 72 h. Then, 20 g of as-prepared sediment was weighed and transferred into a serum bottle and 200 mL of 4NP solution (10 mg L^{-1}, dissolved in 10% methanol, pH 7.0) was added. The samples were kept at 25 °C for 45 days, and the supernatant and sediment were collected at each time interval. Furthermore, the sediments with 30 mg L^{-1} 4NP (at the solid-to-liquid ratio of 1 : 10) were also kept at 5, 15, 25 and 35 °C to investigate 4NP sedimentation and degradation, simulating the seasonal temperature variation in Changsha.

2.3. 4NP extraction and analysis

4NP concentrations were extracted by ultrasonic extraction with the addition of acetone and *n*-hexane (1 : 1, v/v) solution.[26] Sediments (2.0 g) were extracted by adding 15 mL extracting solution and ultrasonic extraction for 30 min. The supernatant was collected by centrifugation at 4 °C. The ultrasonic extraction process was repeated three times, and the supernatant was mixed. The supernatant was removed by rotary evaporation and then, 1 mL of methyl alcohol was added to dilute the extracted 4NP. 4NP concentration was determined by HPLC equipped with a fluorescence detector. Meanwhile, Fe(II) extraction and detection were carried out following the method reported by Li *et al.*[27]

2.4. Sediment enzyme activity analysis

Urease (EC 3.5.1.5) activity was detected using the modified method of Kandeler and Gerber.[28] For urease activity detection, 2.0 g of sediments was mixed with 1 mL methylbenzene for 15 min; then, 2 mL urea solution (100 g L^{-1}) and 4 mL potassium citrate buffer were added and incubated at 38 °C for 24 h before finally adding ultrapure water to a final volume of 25 mL. The supernatant was filtered and the ammonium concentration of the filtered extracts was determined by measuring the absorbance at 578 nm *via* a UV-vis spectrophotometer (UV 2550, Shimadzu). Dehydrogenase activity (EC 1.1.1.1; DHA) was assayed according to the method reported by Tu *et al.*[29] Polyphenol oxidase (EC1.10.3.2, PPO) activity was determined *via* evaluating the oxidation of catechol in the presence of phosphate buffer[30] and expressed as μg of catechol oxidized h^{-1} g^{-1} of sediments (based on dry weight).

2.5. Fe(II) extraction and analysis

Microbially available Fe(II) in sediments was extracted *via* 0.5 M HCl at the solid-to-liquid ratio of 1 : 10.[31] After immediate mixing, the mixture was vibrated at 120 rpm at 30 °C in dark for 24 h. Thereafter, the extraction solution was centrifuged (4000 rpm, 10 min) and filtrated for Fe(II) analysis. The concentrations of Fe(II) were determined by the Fe(II)-selective reagent ferrozine.[32]

2.6. DNA extraction and 16S rRNA high-throughput sequencing analysis

The total genomic DNA was extracted from 0.5 g of wet sediments (sediments with 10 mg L^{-1} 4NP at 30 °C, at days 2, 5, 15 and 30) using the E.Z.N.A. TM Soil DNA kit (Omega Biotek, USA) according to the manufacturer's instructions. PCR amplification was carried out on a MyCycler thermal cycler (Bio-Rad, Hercules, CA, USA) using the forward primer 341F and reverse primer 806R, targeting the V3–V4 hypervariable regions. The purified PCR amplicons were sequenced using the Illumina Miseq (300 bp paired-end reads) platform at Mega Genomics Technology Co., Ltd. (Beijing, China). The sequences were aligned against the SILVA (http://www.arbsilva.de/) database and clustered into operational taxonomic units (OTUs) at 97% similarity. Alpha and beta diversities were then determined using the Quantitative Insights Into Microbial Ecology (QIIME, version 1.6) pipeline.[33] Phylogenetic investigations of communities by reconstruction of unobserved states (PICRUSt) was applied to evaluate the metabolic characteristics of the bacterial communities in the sediments.[34]

2.7. Statistical analysis

Weighted and unweighted UniFrac[35] distances were calculated from the normalized OTU tables for each experiment. α-Diversity values were calculated by the function 'diversity' using the Shannon method in the R package Vegan.[36] Additionally, principal coordinates analysis (PCoA) was used to visualize the variation in the microbial community composition among samples and potential clustering. A metagenomic biomarker discovery approach was employed with LEfSe linear discriminant analysis (LDA) coupled with effect size measurement, which performed a nonparametric Wilcoxon sum-rank test followed by LDA analysis.

3. Results and discussion

3.1. Biodegradation rates of 4NP

In our study, the quick adsorption and sink of 4NP onto sediments were detected. For example, at day 5, the residual 4NP concentration in the aqueous solution was detected to be below 0.05 mg L^{-1} (Fig. 1a). The fast sedimentation of 4NP was perhaps due to its high octanol–water partition coefficient (average $\log K_{ow}$: 4.48) and organic carbon partition coefficient ($\log K_{oc}$: 5.22 ± 0.38),[9] causing the rapid sedimentation of 4NP. This suggested that sediments tended to be the primary environmental sink of 4NP in surface aquatic systems. The results were consistent with those of a previous study: owing to its high hydrophobicity and octanol–water partition coefficient,[9] 4NP tends to be easily adsorbed to soil/sediments, which in turn store it in the environment.

Hence, evaluating the degradation of 4NP in sediments is important for understanding the fate of organic contaminants in an aquatic environment. Fig. 1b shows the dynamic 4NP residual levels in sediments. Almost complete removal was observed at day 45 in sediments incorporated with iron

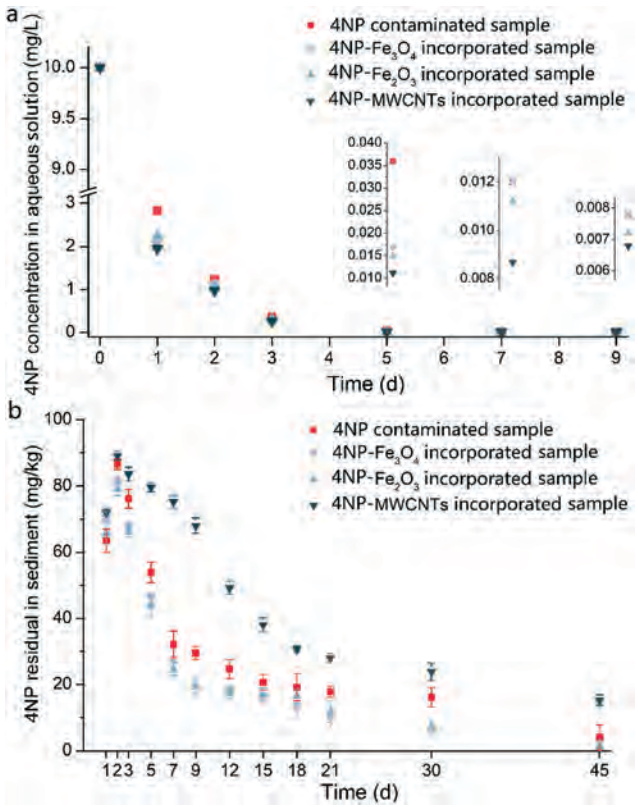

Fig. 1 (a) Residual 4NP concentration in overlying water; (b) residual 4NP concentration in sediments incorporated with different engineered nanomaterials (experimental conditions: initial 4NP concentration: 10 mg L^{-1}; ENM dosage: 0.5%; solid-to-liquid ratio: 1 : 10; temperature: 25 °C, pH: 7.0).

oxides (below 1.0 mg kg^{-1}), whereas 3.97 and 15.26 mg kg^{-1} were observed for sediments without ENMs and with MWCNTs, respectively. Yuan *et al.*[15] reported that the half-lives of 4NP in river sediments varied from 13 to 99 d under aerobic conditions, and 16 bacterial strains capable of aerobically degrading 4NP and NP1EO as carbon sources were isolated. Meanwhile, as shown in Fig. S1,† the residual 4NP concentration in the sediment at 5 °C is higher than those at 15, 25 and 35 °C, suggesting that higher temperatures favored 4NP degradation. At day 8, the residual 4NP levels at 35 °C were 66.95, 20.31, 30.18 and 115.28 mg kg^{-1} accompanied with the degradation efficiencies of 77.68%, 93.23%, 89.94% and 61.57%, respectively.

It was apparent that Fe_3O_4 and Fe_2O_3 nanoparticle incorporation significantly stimulated 4NP degradation. Accordingly, the application of iron oxides to strengthen organic pollution remediation has been widely recognized due to the advantages of their higher chemical activity and good biocompatibility, avoiding environmental and health risks caused by the addition of iron compounds. Hansel *et al.*[37] found that the addition of iron oxides can promote the morphological transformation of valence elements in the environment, thus favoring the degradation of organic matter. Bonneville *et al.*[38] also observed that nano α-Fe_2O_3, amorphous α-Fe_2O_3 and lepidocrocite could be dissolved and transformed by *Shewanella putrefaciens*. Typically, nano α-Fe_2O_3 was first attached to the surface of the bacteria and then reduced to Fe(II) catalyzed by Fe(III) reductase, showing a higher iron reduction rate.

In contrast, MWCNT incorporation limited the 4NP degradation in sediments, with relatively higher residual 4NP levels. Accordingly, the significant inhibition of 4NP degradation might be ascribed to two possible reasons: (i) MWCNTs can act as the carriers of organic contaminants, which may prolong their existence in the environment in case of their lower accessibility to microbes. For instance, Li *et al.*[39] demonstrated that CNTs restrained polyaromatic hydrocarbons by reducing their bio-accessibility in soils, which was quite consistent with our observations. (ii) The potential cytotoxicity and microbial inactivation of MWCNTs might suppress the microbial degradation of 4NP.[40] Microbial inactivation is a theoretical pre-testing indicator of CNT environmental impact and toxicity in soils and sediments. Our previous studies also confirmed that the inactivation of microbial activity and exacerbated microbial inactivation occurred with MWCNTs along with reduced Cd bioavailability.[41] Accordingly, we inferred that the inhibition by MWCNTs for 4NP degradation could be associated with their adsorption ability, resulting in lower bio-accessibility, and their potential toxicity to microbes in the sediments.

3.2. Temporal course of enzyme activity

Commonly, enzymes partially exist in solid or liquid phases of soils in the combined or free state and are involved in the breakdown or oxidation of organic matter.[42,43] In our study, the activities of polyphenol oxidase (PPO), dehydrogenase (DHA) and urease were investigated. As shown in Fig. 2a, the PPO activities in the 4NP-contaminated samples were significantly higher than that of the controls, indicating that PPO activity is stimulated in response to 4NP. The highest PPO activity was observed at day 9 and then, it gradually decreased accompanied by gradual 4NP degradation. In addition, the PPO activity was significantly promoted in Fe_2O_3- and Fe_3O_4-incorporated samples compared to the result for the samples incorporated with MWCNTs. PPO is an important oxidoreductase ubiquitous in soils and sediments contributing to the decomposition and transformation of aromatic compounds.[44] It is also responsible for catalyzing several different phenols to produce *o*-quinones.[29] Thus, the increased PPO activity found could be responsible for the demand-driven degradation of 4NP.

Comparatively, unlike the activity of PPO, the activities of DHA and urease decreased immediately after 4NP contamination. Generally, the activities of urease and DHA reflect the contamination level.[42] As shown in Fig. 2(b and c), the initial 4NP contamination can singularly inhibit DHA and urease activities due to the potential toxicity of 4NP to microorganisms. Previous studies also reported rapid decline in the DHA activity in soils contaminated with heavy metals and organic pollutants.[45] Additionally, the inhibition of DHA and urease decreased with the addition of Fe_3O_4 and Fe_2O_3. MWCNT incorporation represented the most serious and long-duration

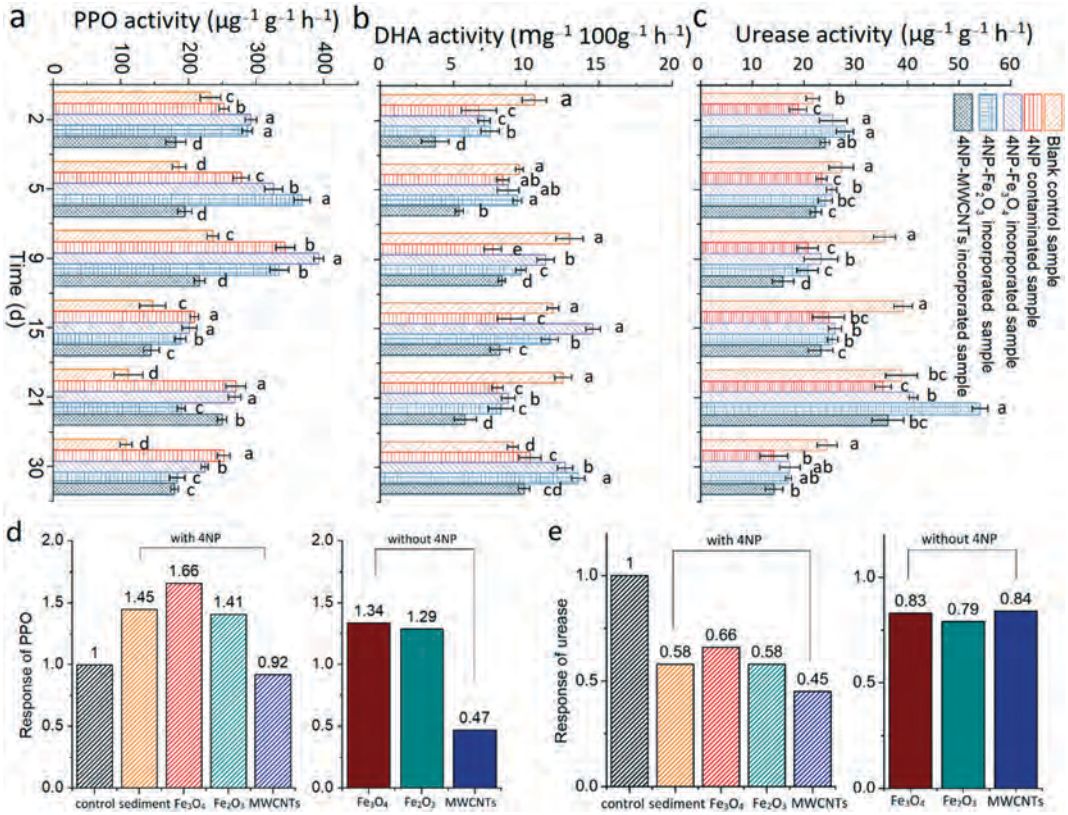

Fig. 2 Dynamic variations in the activity of polyphenol oxidase (PPO, a), dehydrogenase (DHA, b) and urease (c); response of PPO (d) and urease activity (e) to Fe_3O_4 nanoparticles, Fe_2O_3 nanoparticles and MWCNTs at day 9. Different letters indicate significant differences ($p < 0.05$) (experimental conditions: initial 4NP concentration: 10 mg L^{-1}; ENM dosage: 0.5%; solid-to-liquid ratio: 1 : 10; temperature: 25 °C, pH: 7.0).

enzyme inactivation, which possibly depended on the higher residual 4NP level and potential toxicity of MWCNTs.

Considering the potential microbial toxicity of ENMs, a direct comparison of the impacts on enzyme activity (PPO and urease) was conducted with iron oxides and MWCNT incorporation. As shown in Fig. 2d, MWCNTs inhibit the PPO activity, with the activity changing in response below 0.5, while the addition of Fe_3O_4 and Fe_2O_3 nanoparticles elevates the PPO activity in sediments. Similar results were found for urease activity, where MWCNTs were more toxic than iron oxides. The results were consistent with previous observations, showing that MWCNT exposure inhibited microbial biomass, respiration and enzyme activities in soils and sediments.[46] In contrast, iron oxide nanoparticles were much more environmentally friendly with good biocompatibility.[3] Accordingly, we speculated that the variation in microbial enzyme activities in our study was mainly affected in two ways: one by influencing the 4NP degradation pathway and the other *via* the intrinsic fate of iron oxide nanoparticles and MWCNTs.

3.3. Bacterial community composition and individual taxon abundance

For the in-depth understanding of the microbial variation in the sediments, pyrosequencing was used with 16S rRNA-specific oligonucleotide primers. A mean of 69 235 clean tags was obtained. The total numbers of OTUs in the five different groups were 12 793, 17 517, 17 434, 17 645 and 16 446 for groups A, B, C, D and E, respectively (Fig. S2†). There were noteworthy overlaps in the differentially abundant OTUs. The similar OTUs among the five groups were about 6926, and the unique OTUs in groups A, B, C, D and E were 799, 886, 752, 1023 and 685, respectively. Further analysis of the OTUs in the tested samples showed that the core OTUs shared in all 20 samples were 832 (Fig. 3a) with the increase in the observed species in response to 4NP contamination. The samples at day 2 and 5 exhibited the most abundant unique OTUs in the 4NP-contaminated samples. Furthermore, the decrease in the total and unique OTUs in the MWCNT-incorporated samples suggested a possible microbial inhibitory role of MWCNTs.

The PCoA plot based on weighted UniFrac distances suggested that the bacterial community structure varied significantly among 4NP-contaminated samples and the blank control (Fig. 3b). Additionally, within-sample diversity (α-diversity) revealed variation in the five groups (Fig. 3c). The lowest number of the observed species was observed in the blank control, while 4NP contamination elevated the number of observed species greatly. Chao1 and Shannon index analyses further demonstrated that 4NP contamination contributed to significant promotion of bacterial biodiversity. The results suggested

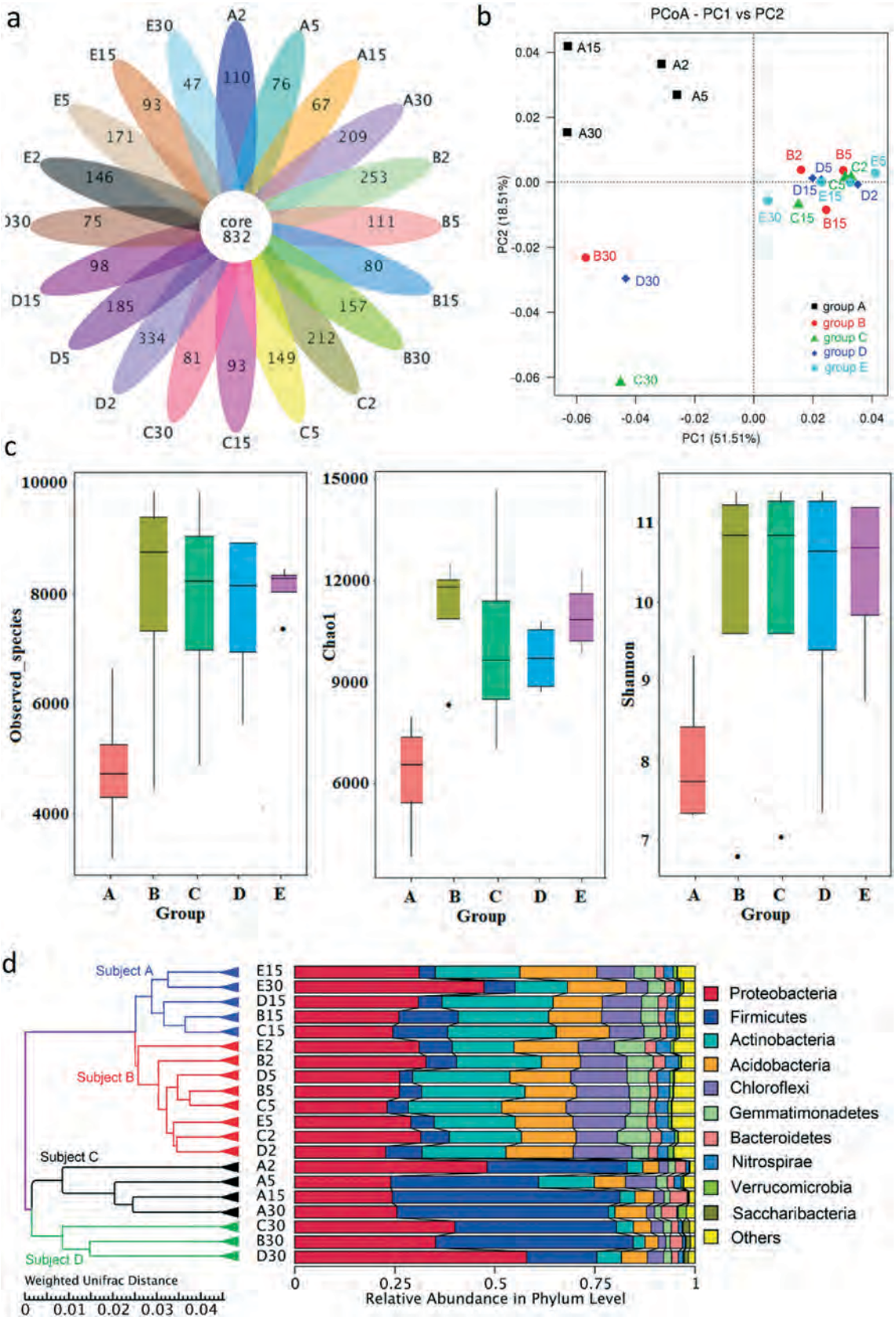

Fig. 3 (a) OTU analysis in the tested samples at day 2, 5, 15 and 30; (b) α-diversity analysis in the five tested groups; (c) PCoA analysis based on the distance of weighted UniFrac; (d) hierarchical cluster analysis based on weighted UniFrac distance in phylum level in the tested samples (group A: control samples without 4NP and ENMs; group B: samples contaminated with 4NP; group C: samples incorporated with 4NP and Fe_3O_4; group D: samples incorporated with 4NP and Fe_2O_3; group E: samples incorporated with 4NP and MWCNTs).

that 4NP contamination stimulated bacterial growth, resulting in a richer bacterial biodiversity. No significant differences were found in the 4NP-contaminated sediments incorporated with Fe_2O_3, Fe_3O_4 or MWCNTs.

Phylogenetic analysis assigned the 16S rRNA gene sequences to different taxa, allowing us to further explore the dynamics of the bacterial community (Fig. 3d). The taxonomic distributions of each bacterial sample were determined at the phylum and genus levels. Apparently, phyla distributions were markedly different among 20 tested samples. The samples could be simply classified into four subjects. In detail, subject A included samples with 4NP contamination at day 15 (also including the MWCNT-incorporated sample at day 30). Subject B involved the samples with relatively high 4NP levels at initial days 2 and 5. Subject C was classified as the samples without 4NP contamination (blank controls), while subject D contained samples with 4NP contamination at day 30 (except for samples with MWCNTs). The results demonstrated that 4NP contamination significantly altered the bacterial communities.

Apparently, *Proteobacteria* were the dominant phylum and did not vary significantly in all samples, which is indicative of their remarkable tolerance to stress relative to 4NP. In subject C, *Proteobacteria* and *Firmicutes* dominated the community, accounting for over 70% of all the sequences generated. *Firmicutes* are the most abundant phylum in natural sediments with a relatively stable proportion of 36.86–56.81%. Interestingly, the initial 4NP exposure (day 2, 5 and 15) led to a significant decrease in the proportion of *Firmicutes* to below 17%. Meanwhile, we also observed the recovery of *Firmicutes* at day 30 with 4NP degradation (except for samples with MWCNTs with high levels of 4NP). In subjects A and B with high levels of 4NP, *Proteobacteria* (22.72–35.19%), *Actinobacteria* (15.46–27.76%) and *Acidobacteria* (9.78–19.22%) were the most abundant groups. Furthermore, *Actinobacteria*, *Acidobacteria*, *Chloroflexi* and *Gemmatimonadetes* increased significantly in response to 4NP contamination. The results indicated the vital roles of these bacteria in organic tolerance and degradation in sediments. Notably, *Acidobacteria*, which have been reported to be abundant in soils and sediments, were characterized by their ability to withstand metal-contaminated, organic-contaminated, acidic, and other extreme environments.[47] Previous studies also reported the role of *Acidobacteria* in the microbial degradation of lignocellulosic plant biomass.[48,49] Moreover, recent studies have reported that the members of *Chloroflexi* are ubiquitous in the environment, and some of them play important roles in organic matter degradation.[50] The large proportion and stimulation in these phyla are indicators of their contribution to biodegradation.[51]

Further comparison of the bacterial communities was conducted at the class level to investigate the impact of 4NP contamination and ENM incorporation (ESI,† Fig. S3). A comparison between groups A and B revealed that 4NP contamination led to sharp decrease in *Bacilli*, *Clostridia*, *Spartobacteria*, *Betaproteobacteria*, *Bacteroidia* and *Sphingobacteriia*, suggesting their sensitivity to 4NP contamination owing to potential toxicity. In group B, *Gammaproteobacteria* and *Flavobacteria* were observed to be in the highest abundance. Meanwhile, the comparison among three groups with ENMs revealed that *Negativicutes*, *Acidobacteria*, *Caldilineae*, *Themomicrobia* and *Ktedonobacteria* were the dominant classes in groups C and D with iron oxide nanomaterials, whereas the most represented bacterial classes in group E were Soil Crenarchaeotic Group (SCG), *α-proteobacteria*, *Deinococci* and *Phycisphaerae*. Although the dominant classes varied among the treatments, most bacterial classes were shared by all sediments. For example, *Nitrospira*, *Chloroflexia*, *Acidimicrobiia*, *Acidobacteria*, *Gemmatimonadetes* and *Thermoleophilia* significantly increased in response to 4NP contamination but did not vary significantly with various ENM incorporations. These bacteria were also widely reported to be involved in the degradation of organic contaminants and to have the potential ability to withstand other numerous contaminants,[52–54] which may reflect the ecological coherence of the contaminated sediments.

3.4. Discriminative bacterial community analysis

To identify the taxa that differed significantly among the 4NP-contaminated samples, linear discriminant analysis effect size (LEfSe) was employed. As shown in Fig. 4, 16 bacterial clades present statistically significant differences with an LDA threshold of 2.0. Most bacteria were significantly enriched in group E with MWCNTs, while only 1 and 2 clades showed favored abundances in groups C and D, respectively. For example, higher taxonomic levels of *Thermales* (including *Deinococcus*, *Deinococci*, *Thermales*, *Thermaceae* and *Thermus*), *Phycisphaerae*, *Halieaceae*, *Flavitalea* and *Nitrosococcus* were found in group E (Fig. 4a). Commonly, *Deinococcus*, *Thermus* and *Nitrosococcus* are known to be capable of degrading phenolic compounds.[55] Thus, the dominance of these species indicated that they may have important functions in biodegradation. However, although consistently observed in contaminated environments, no significant roles in organic contaminant biodegradation were found for *Halieaceae*, *Phycisphaerae* and *Flavitalea*.

It was noteworthy that *Nocardia* was the dominant genus as well as the biomarker in group C with Fe_3O_4 nanoparticles, while *Pantoea* and *Promicromonospora* were significantly more abundant in group D with Fe_2O_3 nanoparticles. *Nocardia*, *Pantoea* and *Promicromonospora* species have been widely reported as candidates for the removal of organic contaminants. Notably, *Nocardia* and *Promicromonospora* are actinobacterial[56] and play important roles as the recyclers of organic matter.[57] Typically, *Nocardia* has been reported to synthesize biosurfactants, such as lipopeptides and glycolipids, which are beneficial for the potential degradation of hydrocarbon compounds.[58] Chang *et al.*[59] isolated *Nocardia* sp. strain CYKS2 capable of degrading dibenzothiophene and thiazole. Zeinali *et al.*[60] also reported that *Nocardia otitidiscaviarum* TSH1 could degrade phenol, *n*-alkanes and some polycyclic aromatic hydrocarbons. Their predominance

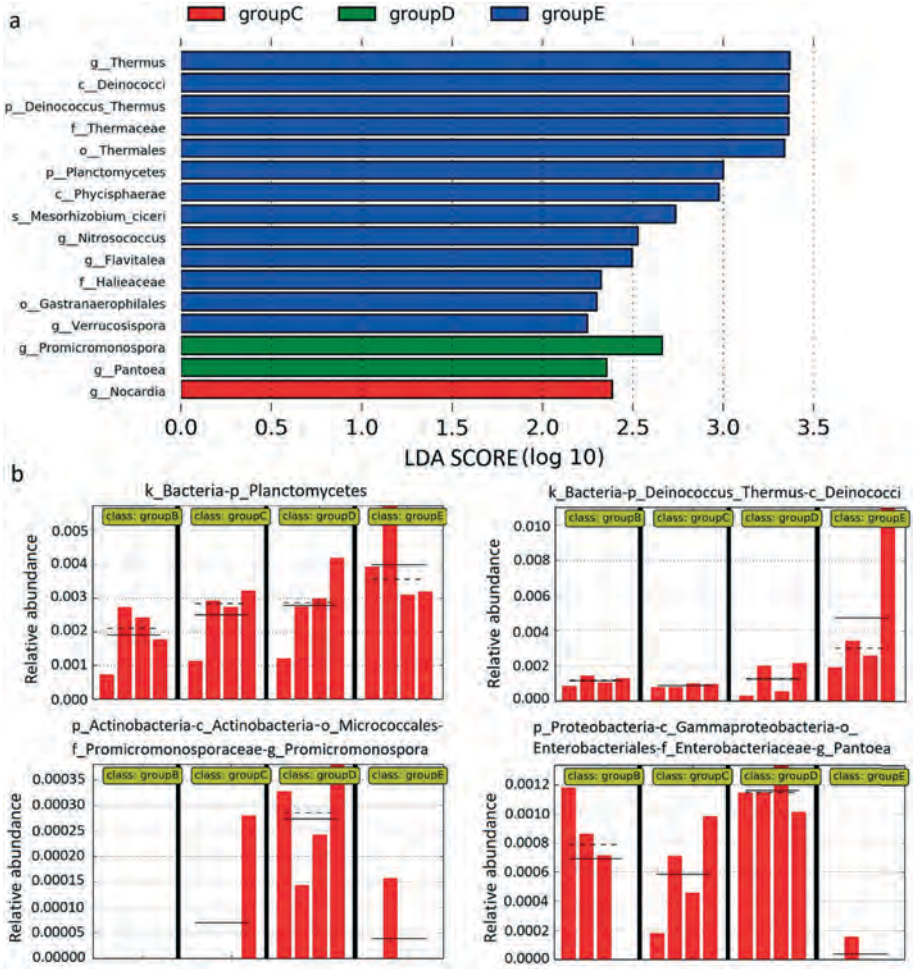

Fig. 4 LEfSe results (a) and biomarker detection analysis of bacteria among the four tested groups (b) (group B: samples contaminated with 4NP; group C: samples incorporated with 4NP and Fe_3O_4; group D: samples incorporated with 4NP and Fe_2O_3; group E: samples incorporated with 4NP and MWCNTs).

in groups C and D suggested that they were selectively enriched by iron oxide incorporation and exhibited an important function related to 4NP removal.

Considering the significant difference in 4NP degradation, LEfSe analysis was further conducted between groups D and E (group D *vs.* group E). LefSe analysis showed biomarkers demonstrating significant differences between group D and group E. As shown in Fig. S4,† group E with MWCNTs mainly enriched members of *Flavitalea*, *Lysobacter*, *Deinococcus*, and *Oligoflexales*, which was consistent with previous results (Fig. S4†). *Enterobacteriales* (o) (including *Enterobacteriaceae* (f) and *Enterobacteriales* (g)), *Promicromonospora* (g), and *Aquincola* (g) were the discriminative taxa in group D with Fe_2O_3 nanoparticles. Interestingly, iron-reducing bacteria, including *Pantoea*, *Shewanella* and *Shewanellaceae*, were discriminately detected in group D. It may be speculated that iron-reducing bacteria proliferate in response to Fe_2O_3 nanoparticle incorporation. These iron-reducing bacteria, which are capable of coupling microbial Fe(III) reduction to the oxidation of organic matter, play a significant role in global geochemical cycling.[61,62] *Pantoea* and *Shewanellaceae* families are well-known ferric iron-respiring microorganisms (FRMs), which use Fe(III) as well as other metals as terminal electron acceptors.[63] Accordingly, FRMs such as *Pantoea*,[64] *Salinibacterium*[65] and *Shewanella*[66] have been reported to be capable of transforming, detoxifying, or immobilizing a variety of metallic and organic pollutants. For example, *Pantoea* bacterium, such as *P. agglomerans* SP1, is widely reported to participate in microbial Fe(III) reduction[67] and is linked to the biodegradation of numerous organic contaminants.[68,69] Recently, Haleyur *et al.*[64] reported that *Pantoea* sp. could also utilize substrates from different biochemical categories (*i.e.*, amino acids, phenolic compounds, carbohydrates, carboxylic acids and polymers) as carbon sources. This suggested that iron oxide incorporation induced microorganisms with iron-reducing ability and endowed a better advantage in 4NP survival and degradation.

3.5. Predicted functions based on PICRUSt analysis

We also explored microbial functions using the PICRUSt algorithm.[34] A total of 6372 KEGG functions corresponding to

304 level 3 KO entries were identified by matching sequence data based on KEGG enzyme nomenclature. The majority of predicted protein sequences in the tested samples were associated with the functions involved in metabolism (48.87–52.04%), genetic information processing (15.68–16.03%), environmental information processing (12.82–15.31%) and unclassified processes (13.06–13.40%) (Fig. 5a). Specifically, 4NP contamination resulted in significant increase in the genes involved in relevant metabolic functions, including amino acid metabolism (9.78–11.41%), carbohydrate metabolism (9.38–10.83%), energy metabolism (5.27–6.03%), xenobiotic biodegradation and metabolism (2.87–4.64%), and replication and repair (6.47–7.31%), whereas enzyme families (1.89–2.15%), cell mobility (2.88–4.60%) and membrane transport (4.22–5.95%) were significantly depleted in response to 4NP contamination (Fig. 5b). The results demonstrated that 4NP contamination promoted genes for metabolism, genetic information processing, environmental information processing and cellular processes associated with biodegradation pathways. Meanwhile, Fe_2O_3-

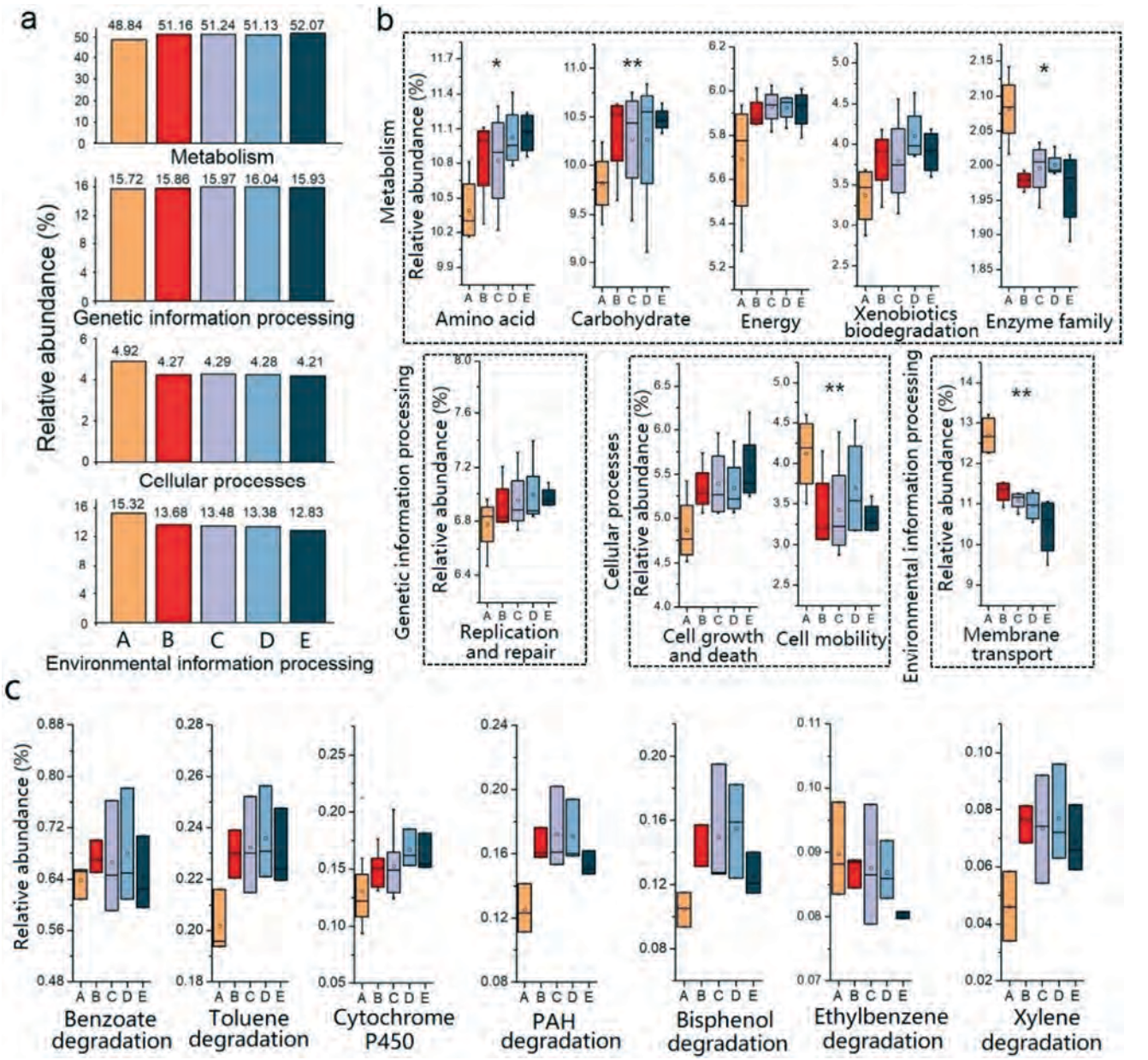

Fig. 5 (a) Variation of bacterial functions related to metabolism, genetic information processing, cellular processes and environmental information processing at KEGG level 1; (b) variation of bacterial functions at KEGG level 2; (c) variation of bacterial functions related to xenobiotic biodegradation and metabolism at KEGG level 3. Bacterial gene functions were predicted from 16S rRNA gene-based microbial compositions using the PICRUSt algorithm to make inferences from KEGG annotated databases (group A: control samples without 4NP and ENMs; group B: samples contaminated with 4NP; group C: samples incorporated with 4NP and Fe_3O_4; group D: samples incorporated with 4NP and Fe_2O_3; group E: samples incorporated with 4NP and MWCNTs).

incorporated samples showed the most significant expression in the genes related to carbohydrate metabolism (10.83%) and membrane transport (5.95%). In contrast, MWCNT incorporation repressed these functional genes while promoting the genes associated with amino acid metabolism and cell growth- and death-related pathways.

Typically, 4NP contamination significantly enriched the abundances of xenobiotic biodegradation pathways, including the degradation of polycyclic aromatic hydrocarbons, benzoate, bisphenol, xylene and drug metabolism (Fig. 5c). Specifically, the samples incorporated with Fe_2O_3 nanoparticles possessed the most abundant functional genes corresponding to organic degradation, followed by the samples with Fe_3O_4 nanoparticles, while those with MWCNTs showed the least functional genes. The results demonstrated that ENMs affected bacterial function in cellular processes and metabolic pathways, thus also affecting the 4NP degradation ability in sediments. The results agreed with those reported by Kim *et al.*,[70] who reported that $Fe(OH)_3$ addition increased cell numbers/viability and caused changes in cellular physiology; this resulted in the enhancement of carbon tetrachloride bioremediation mainly *via* stimulating microbial iron reduction and surface-bound Fe(II) production.

Additionally, it was interesting to note that the proteins related to iron regulation and transport also varied significantly among different groups. In responding to the changes in the environment, especially to iron oxide incorporation, response regulators usually alter the expression of genes that promote iron transport and availability. Here, these related functional proteins were determined by PICRUSt prediction and are presented in Fig. 6a. As is well-known, iron is the most abundant transition metal in the environment and is an essential co-factor for many metabolic enzymes involved in biological reactions.[61] Commonly, iron transport is usually controlled *via* the ferrous iron transport system (composed of three proteins FeoA, FeoB and FeoC) and iron complex transport system having a substrate binding protein, iron complex out-membrane receptor protein, permease protein and ATP binding protein.[66] Meanwhile, ABC transporters can also translocate heme and iron-siderophores across the cytoplasmic membrane with important functions in iron metabolism.[71] Meanwhile, iron uptake is usually regulated by the ferric uptake regulator (Fur) and Fur-like proteins (including manganese uptake regulator (Mur) and peroxide stress response (PerR)). The diphtheria toxin regulator (DtxR) protein can also regulate the iron uptake in some Gram-positive bacteria (*streptomyces*, *corynebacteria*, *mycobacteria*, *etc.*).[62,65] As shown in Fig. 6a, the iron complex transport system comprising permease protein, out-membrane receptor protein and substrate-binding protein widely varied in all samples. The mean percentage of these iron complex transport systems in group C with Fe_2O_3 nanoparticles was higher than that in group E with MWCNTs. It was apparent that iron oxide incorporation promoted the expressions of Fur family transcriptional proteins, diphtheria toxin regulators (including Fur, FhuF and DtxR) and the iron complex transport system

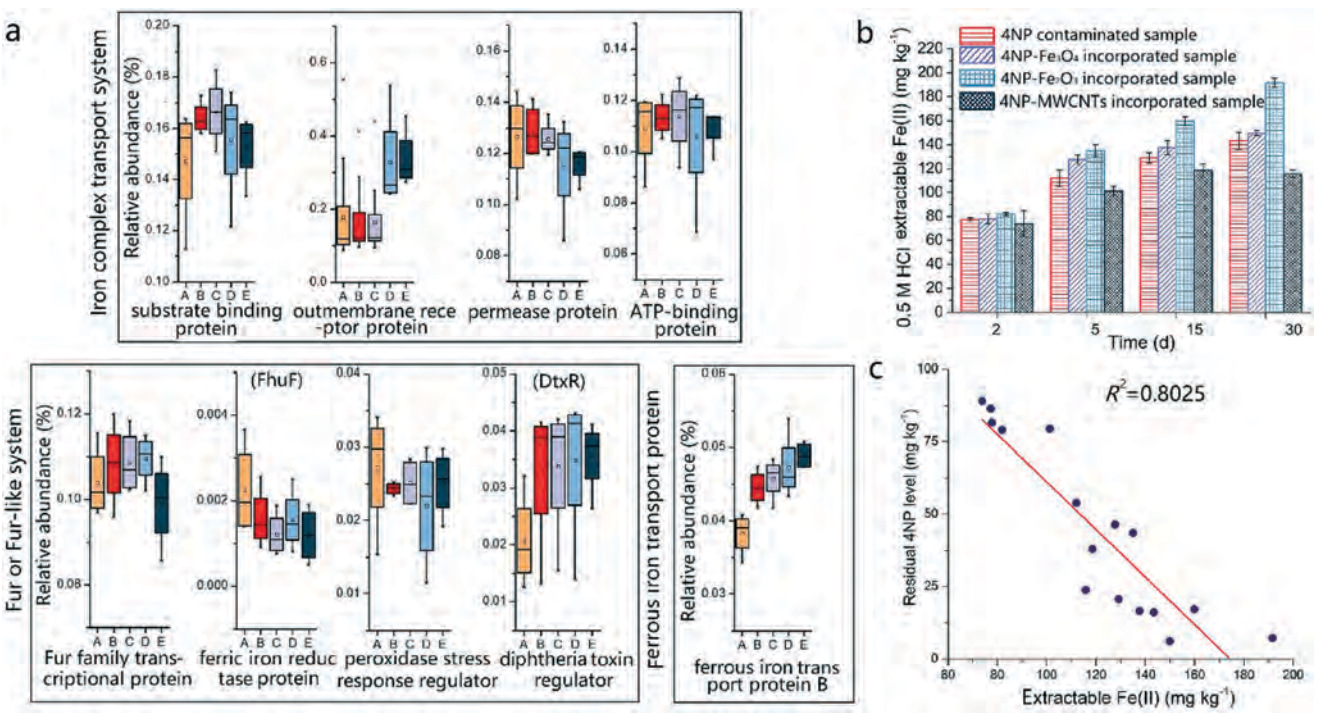

Fig. 6 (a) Variation of bacterial functions relating to iron regulated proteins (group A: control samples without 4NP and ENMs; group B: samples contaminated with 4NP; group C: samples incorporated with 4NP and Fe_3O_4; group D: samples incorporated with 4NP and Fe_2O_3; group E: samples incorporated with 4NP and MWCNTs); (b) HCl-extracted Fe(II) concentration in sediments; (c) Relationship between residual 4NP concentration and HCl-extracted Fe(II) concentrations.

(especially substrate-binding protein, permease protein and ATP-binding protein) (Fig. 6a), which are responsible for iron transport and iron cycling in the environment. However, PICRUSt is only a means of predicting functional genes; thus, further research is required to confirm the accuracy of gene function information by other biology technologies.

To date, limited studies are available on the effects of exogenous iron oxide nanomaterial incorporation on the iron regulation pathway and iron cycling in natural sediments. Thus, to deepen the understanding of the possible roles of iron oxide incorporation and iron reduction in 4NP degradation, microbial available Fe(II) concentrations in sediments were determined (Fig. 6b). Apparently, gradual increase in microbial available Fe(II) was found in all samples. In natural sediments without ENMs, the Fe(II) concentration was elevated from 77.26 mg kg^{-1} to 140.42 mg kg^{-1}, which could possibly be due to natural iron oxides in river sediments undergoing reduction with increasingly available Fe(II).[72] Indeed, significant increase in the Fe(II) levels was found in groups C and D with iron oxide incorporation, while the sediments incorporated with MWCNTs exhibited the lowest Fe(II) levels during the entire duration of the 30 day study. The results demonstrated that iron oxide nanoparticle incorporation stimulated iron transport and cycling in sediments. The observations were similar to those of previous studies reporting that the microbial reduction of Fe(III) to Fe(II) has key roles in the iron cycle and organic matter mineralization in the overlying water–sediment interface.[73] Accordingly, iron oxides could be dissolved in soil or sediment to form Fe(III) and could be further reduced to Fe(II) *via* microbial reduction by anaerobic, facultative anaerobic and hyperthermophilic microorganisms. Insoluble Fe(III) oxides are generally the most abundant potential electron acceptors for the oxidation of organic matter. In detail, iron-reducing microbes can transfer electrons to the extracellular surface of iron oxides by respiration; Fe(III) acts as the electron acceptor and is converted to Fe(II). Meanwhile, microbially driven Fenton reactions might occur with the alternate production of H_2O_2 (*via* microbial O_2 respiration) and Fe(II) (*via* microbial Fe(III) reduction), which might promote the degradation of organics[74] through the cyclic transformation between Fe(III) and Fe(II).[75]

In our study, significant negative correlation was found between residual 4NP levels and Fe(II) concentrations in the sediments (Fig. 6c), suggesting the coherence of lower residual 4NP and higher Fe(II) levels. The results agreed with those of previous studies: crystalline iron oxides, including goethite and hematite, can stimulate iron reduction and organic degradation.[76] Although the thermodynamic favorability of crystalline Fe(III) oxide reduction increased compared to that of amorphous Fe(III) oxides, previous studies have suggested that FRMs are capable of utilizing crystalline solid-phase Fe(III) as the electron acceptor.[73,77] For example, Zhang *et al.*[78] also found that a variety of iron oxide-mediated iron reduction processes significantly promoted the reduction of nitrate by *Bacillus* sp., among which α-Fe_2O_3 and γ-Fe_2O_3 exhibited the most notable enhancement. Meanwhile, even with weak Fe(III) reduction ability, many fermentative microorganisms were reported to be responsible for the production of fermentation products, serving as electron donors for iron reduction.[75] For example, *Shewanella* species can transfer electrons from the cell surface to Fe(III) oxides by releasing soluble electron-shuttling compounds, thus overcoming the insolubility of Fe(III) oxides.[38] Furthermore, redox-reactive organic compounds ubiquitous in sediments, such as humic acids and plant exudates, can also serve as electron shuttles, which can transfer electrons between a wide variety of both inorganic and organic compounds in redox reactions.[79] These findings were consistent with those of the LEfSe analysis, which showed that *Shewanella* species tended to be biomarkers in Fe_2O_3-incorporated sediments. Herein, the results suggested that such an enhancement in microbial-mediated hematite-Fe(III) reduction to microbial available Fe(II) might contribute to the promotion of 4NP degradation. Accordingly, we inferred that iron oxide nanomaterial-promoted 4NP degradation might be attributed to two possible reasons: firstly, good biocompatibility of iron oxides led to lower toxicity to sediment microbes; secondly, the exogenous addition of iron oxides might increase the viability of iron reducing microbes which use Fe(III) as electron acceptors, thus stimulating microbial iron reduction and promoting 4NP degradation.

4. Conclusion

Unlike cellular toxicity studies, which have been widely performed, studies focusing on the environmental behavior and fate of ENMs are still in their infancy. Investigations on the interactions among ENMs, chemicals and environmental organisms remain challenging. In this study, taking 4NP as a target contaminant, we explored 4NP sedimentation, degradation and bacterial response in a water–sediment interface ecosystem. We found the following conclusions:

- Of the three kinds of ENMs used here, iron oxides promoted 4NP degradation in sediments, whereas MWCNTs significantly inhibited 4NP degradation.
- The observed bacterial response and LEfSe analysis results suggested that iron oxide incorporation stimulated iron-respiring bacteria participating in iron reduction, thus enhancing 4NP degradation.
- PICRUSt analysis demonstrated that iron oxides elevated the expressions of xenobiotic biodegradation, metabolism proteins, iron-regulated proteins, including FeoB, Fur and Fur-like proteins, and iron complex transport systems. Indeed, such enhanced expressions might contribute to the promotion of 4NP degradation in iron oxide-incorporated sediments. In contrast, the reduction in these functional proteins and severe microbial inactivation impeded 4NP degradation in MWCNT-incorporated sediments.
- Given this information, we suggested that the good biocompatibility and stimulation in the predominance of iron-reducing bacteria probably had important functions in sediments and resulted in a better performance in 4NP degradation.

• Further studies are required to confirm the accuracy of gene function information by biology technologies (*e.g.*, metagenomics, microarrays, single-cell genomics).

Conflicts of interest

There are no conflicts to declare.

Acknowledgements

This study was financially supported by the Program for the National Natural Science Foundation of China (51709101, 51879101, 51609023, 51579098, 51779090, 51709101, 51521006), the National Program for Support of Top–Notch Young Professionals of China (2014), the Program for Changjiang Scholars and Innovative Research Team in University (IRT-13R17), and Hunan Provincial Science and Technology Plan Project (2018SK20410, 2017SK2243, 2016RS3026), and the Fundamental Research Funds for the Central Universities (531118010226, 531119200086, 531118010114, 531107050978).

References

1 D. Singh, L. A. Schifman, C. Watson-Wright, G. A. Sotiriou, V. Oyanedel-Craver, W. Wohlleben and P. Demokritou, Nanofiller presence enhances polycyclic aromatic hydrocarbon (PAH) profile on nanoparticles released during thermal decomposition of nano-enabled thermoplastics: potential environmental health implications, *Environ. Sci. Technol.*, 2017, **51**(9), 5222–5232.

2 J. H. Deng, X. R. Zhang, G. M. Zeng, J. L. Gong, Q. Y. Niu and J. Liang, Simultaneous removal of Cd (II) and ionic dyes from aqueous solution using magnetic graphene oxide nanocomposite as an adsorbent, *Chem. Eng. J.*, 2013, **226**, 189–200.

3 P. Xu, G. M. Zeng, D. L. Huang, C. L. Feng, S. Hu, M. H. Zhao, C. Lai, Z. Wei, C. Huang and G. X. Xie, Use of iron oxide nanomaterials in wastewater treatment: A review, *Sci. Total Environ.*, 2012, **424**, 1–10.

4 X. Tan, Y. Liu, G. Zeng, X. Wang, X. Hu, Y. Gu and Z. Yang, Application of biochar for the removal of pollutants from aqueous solutions, *Chemosphere*, 2015, **125**, 70–85.

5 A. Parish, *Production and applications of carbon nanotubes, carbon nanofibers, fullerenes, graphene and nanodiamonds: A global technology survey and market analysis*, ET-113, Innovative Research and Products, Stamford, CT, USA, 2011.

6 A. Nel, T. Xia, L. Mädler and N. Li, Toxic potential of materials at the nanolevel, *Science*, 2006, **311**(5761), 622–627.

7 V. L. Colvin, The potential environmental impact of engineered nanomaterials, *Nat. Biotechnol.*, 2003, **21**, 1166.

8 T. Hofmann and F. von der Kammer, Estimating the relevance of engineered carbonaceous nanoparticle facilitated transport of hydrophobic organic contaminants in porous media, *Environ. Pollut.*, 2009, **157**(4), 1117–1126.

9 A. Soares, B. Guieysse, B. Jefferson, E. Cartmell and J. N. Lester, Nonylphenol in the environment: A critical review on occurrence, fate, toxicity and treatment in wastewaters, *Environ. Int.*, 2008, **34**(7), 1033–1049.

10 J. Shan, T. Wang, C. Li, E. Klumpp and R. Ji, Bioaccumulation and bound-residue formation of a branched 4-nonylphenol isomer in the geophagous earthworm Metaphire guillelmi in a rrice paddy soil, *Environ. Sci. Technol.*, 2010, **44**(12), 4558–4563.

11 Overview of the US nonylphenol sector, *Anonymous, Focus Surfact.*, 2007, vol. 8, p. 4.

12 T. Toyama, M. Murashita, K. Kobayashi, S. Kikuchi, K. Sei, Y. Tanaka, M. Ike and K. Mori, Acceleration of nonylphenol and 4-tert-octylphenol degradation in sediment by *Phragmites australis* and associated rhizosphere bacteria, *Environ. Sci. Technol.*, 2011, **45**(15), 6524–6530.

13 W. Giger, P. H. Brunner and C. Schaffner, 4-Nonylphenol in sewage sludge: accumulation of toxic metabolites from nonionic surfactants, *Science*, 1984, **225**(4662), 623.

14 G. G. Ying, B. Williams and R. Kookana, Environmental fate of alkylphenols and alkylphenol ethoxylates-a review, *Environ. Int.*, 2002, **28**(3), 215–226.

15 S. Yuan, C. Yu and B. Chang, Biodegradation of nonylphenol in river sediment, *Environ. Pollut.*, 2004, **127**(3), 425–430.

16 K. Fujii, N. Urano, H. Ushio, M. Satomi and S. Kimura, *Sphingomonas cloacae* sp. nov., a nonylphenol-degrading bacterium isolated from wastewater of a sewage-treatment plant in Tokyo, *Int. J. Syst. Evol. Microbiol.*, 2001, **51**(2), 603–610.

17 W. Pluemsab, Y. Fukazawa, T. Furuike, Y. Nodasaka and N. Sakairi, Cyclodextrin-linked alginate beads as supporting materials for *Sphingomonas cloacae*, a nonylphenol degrading bacteria, *Bioresour. Technol.*, 2007, **98**(11), 2076–2081.

18 A. Soares, B. Guieysse, O. Delgado and B. Mattiasson, Aerobic biodegradation of nonylphenol by cold-adapted bacteria, *Biotechnol. Lett.*, 2003, **25**(9), 731–738.

19 J. H. Writer, J. N. Ryan, S. H. Keefe and L. B. Barber, Fate of 4-nonylphenol and 17β-estradiol in the Redwood River of Minnesota, *Environ. Sci. Technol.*, 2011, **46**(2), 860–868.

20 H. Wu, C. Lai, G. Zeng, J. Liang, J. Chen, J. Xu, J. Dai, X. Li, J. Liu and M. Chen, The interactions of composting and biochar and their implications for soil amendment and pollution remediation: a review, *Crit. Rev. Biotechnol.*, 2017, **37**(6), 754–764.

21 R. Margesin, A. Zimmerbauer and F. Schinner, Monitoring of bioremediation by soil biological activities, *Chemosphere*, 2000, **40**(4), 339–346.

22 X. Ren, G. Zeng, L. Tang, J. Wang, J. Wan, Y. Liu, J. Yu, H. Yi, S. Ye and R. Deng, Sorption, transport and biodegradation–an insight into bioavailability of persistent organic pollutants in soil, *Sci. Total Environ.*, 2018, **610**, 1154–1163.

23 P. Xu, G. M. Zeng, D. L. Huang, M. Yan, M. Chen, C. Lai, H. Jiang, H. P. Wu, G. M. Chen and J. Wan, Fabrication of reduced glutathione functionalized iron oxide nanoparticles for magnetic removal of Pb (II) from wastewater, *J. Taiwan Inst. Chem. Eng.*, 2017, **71**, 165–173.

24 J. L. Gong, B. Wang, G. M. Zeng, C. P. Yang, C. G. Niu, Q. Y. Niu, W. J. Zhou and Y. Liang, Removal of cationic dyes from aqueous solution using magnetic multi-wall carbon

nanotube nanocomposite as adsorbent, *J. Hazard. Mater.*, 2009, **164**(2), 1517–1522.

25 J. Wan, G. Zeng, D. Huang, L. Hu, P. Xu, C. Huang, R. Deng, W. Xue, C. Lai and C. Zhou, Rhamnolipid stabilized nanochlorapatite: Synthesis and enhancement effect on Pb-and Cd-immobilization in polluted sediment, *J. Hazard. Mater.*, 2018, **343**, 332–339.

26 P. Xu, C. Lai, G. Zeng, D. Huang, M. Chen, B. Song, X. Peng, J. Wan, L. Hu, A. Duan and W. Tang, Enhanced bioremediation of 4-nonylphenol and cadmium co-contaminated sediment by composting with *Phanerochaete chrysosporium* inocula, *Bioresour. Technol.*, 2018, **250**(Supplement C), 625–634.

27 X. Li, S. Zhou, F. Li, C. Wu, L. Zhuang, W. Xu and L. Liu, Fe(III)oxide reduction and carbon tetrachloride dechlorination by a newly isolated *Klebsiella pneumoniae* strain L17, *J. Appl. Microbiol.*, 2009, **106**, 130–139.

28 E. Kandeler and H. Gerber, Short term assay of soil urease activity using colorimetric determination of ammonium, *Biol. Fertil. Soils*, 1988, **6**, 68–72.

29 C. Tu, Y. Teng, Y. Luo, X. Sun, S. Deng, Z. Li, W. Liu and Z. Xu, PCB removal, soil enzyme activities, and microbial community structures during the phytoremediation by alfalfa in field soils, *J. Soils Sediments*, 2011, **11**(4), 649–656.

30 P. Perucci, C. Casucci and S. Dumontet, An improved method to evaluate the o-diphenol oxidase activity of soil, *Soil Biol. Biochem.*, 2000, **32**(13), 1927–1933.

31 S. Ratering and S. Schnell, Localization of iron-reducing activity in paddy soilby profile studies, *Biogeochemistry*, 2000, **48**(3), 341–365.

32 H. Fadrus and J. Malý, Rapid extraction-photometricdetermination of traces of iron(II) and iron (III) in water with 1, 10-phenanthroline, *Anal. Chim. Acta*, 1975, 77, 315–316.

33 J. G. Caporaso, J. Kuczynski, J. Stombaugh, K. Bittinger, F. D. Bushman, E. K. Costello, N. Fierer, A. G. Peña, J. K. Goodrich, J. I. Gordon, G. A. Huttley, S. T. Kelley, D. Knights, J. E. Koenig, R. E. Ley, C. A. Lozupone, D. McDonald, B. D. Muegge, M. Pirrung, J. Reeder, J. R. Sevinsky, P. J. Turnbaugh, W. A. Walters, J. Widmann, T. Yatsunenko, J. Zaneveld and R. Knight, QIIME allows analysis of high-throughput community sequencing data, *Nat. Methods*, 2010, **7**, 335.

34 M. G. Langille, J. Zaneveld, J. G. Caporaso, D. McDonald, D. Knights, J. A. Reyes, J. C. Clemente, D. E. Burkepile, R. L. V. Thurber, R. Knight, R. G. Beiko and C. Huttenhower, Predictive functional profiling of microbial communities using 16S rRNA marker gene sequences, *Nat. Biotechnol.*, 2013, **31**, 814–821.

35 C. Lozupone and R. Knight, UniFrac: a new phylogenetic method for comparing microbial communities, *Appl. Environ. Microbiol.*, 2005, **71**(12), 8228–8235.

36 J. Oksanen, R. Kindt, P. Legendre, B. O'Hara, M. H. H. Stevens, M. J. Oksanen and M. Suggests, *The vegan package, Community Ecology Package*, 2007, vol. 10, pp. 631–637.

37 C. M. Hansel, S. G. Benner, P. Nico and S. Fendorf, Structural constraints of ferric (hydr)oxides on dissimilatory iron reduction and the fate of Fe(II), *Geochim. Cosmochim. Acta*, 2004, **68**(15), 3217–3229.

38 S. Bonneville, T. Behrends, P. V. Cappellen, C. Hyacinthe and W. F. M. Roling, Reduction of Fe(III) colloids by Shewanella putrefaciens: A kinetic model, *Geochim. Cosmochim. Acta*, 2006, **70**, 5842–5854.

39 S. B. Li, U. Turaga, B. Shrestha, T. A. Anderson, S. S. Ramkumar, M. J. Green, S. Das and J. E. Cañas-Carrell, Mobility of polyaromatic hydrocarbons (PAHs) in soil in the presence of carbon nanotubes, *Ecotoxicol. Environ. Saf.*, 2013, **96**, 168–174.

40 S. Kang, M. Herzberg and D. F. Rodrigues, Antibacterial effects of carbon nanotubes: Size does matter, *Langmuir*, 2008, **24**(13), 6409–6413.

41 P. Xu, M. Chen, G. Zeng, D. Huang, C. Lai, Z. Wang, M. Yan, Z. Huang, X. Gong, B. Song, T. Li and A. Duan, Effects of multi-walled carbon nanotubes on metal transformation and natural organic matters in riverine sediment, *J. Hazard. Mater.*, 2019, **374**, 459–468.

42 T. Chen, C. Sun, G. Lin and W. Chen in *Change in enzymatic activity in Tween80-enhanced phytoremediation of polychlorinated biphenyl-contaminated soil*, Application of Materials Science and Environmental Materials (AMSEM2015): Proceedings of The 3rd International Conference, 2016, World Scientific, 2016, p. 179.

43 W. Xue, D. Huang, G. Zeng, J. Wan, C. Zhang, R. Xu, M. Cheng and R. Deng, Nanoscale zero-valent iron coated with rhamnolipid as an effective stabilizer for immobilization of Cd and Pb in river sediments, *J. Hazard. Mater.*, 2018, **341**, 381–389.

44 M. Sylvestre, Prospects for using combined engineered bacterial enzymes and plant systems to rhizoremediate polychlorinated biphenyls, *Environ. Microbiol.*, 2013, **115**(3), 907–915.

45 M. B. Hinojosa, J. A. Carreira, J. M. Rodríguez-Maroto and R. García-Ruíz, Effects of pyrite sludge pollution on soil enzyme activities: Ecological dose–response model, *Sci. Total Environ.*, 2008, **396**(2), 89–99.

46 F. Gottschalk, T. Sonderer, R. W. Scholz and B. Nowack, Modeled Environmental Concentrations of Engineered Nanomaterials (TiO_2, ZnO, Ag, CNT, Fullerenes) for Different Regions, *Environ. Sci. Technol.*, 2009, **43**(24), 9216–9222.

47 N. L. Ward, J. F. Challacombe, P. H. Janssen, B. Henrissat, P. M. Coutinho, M. Wu, G. Xie, D. H. Haft, M. Sait and J. Badger, Three genomes from the phylum *Acidobacteria* provide insight into the lifestyles of these microorganisms in soils, *Appl. Environ. Microbiol.*, 2009, **75**(7), 2046–2056.

48 T. A. Pankratov, A. O. Ivanova, S. N. Dedysh and W. Liesack, Bacterial populations and environmental factors controlling cellulose degradation in an acidic *Sphagnum* peat, *Environ. Microbiol.*, 2011, **13**(7), 1800–1814.

49 S. A. Eichorst, C. R. Kuske and T. M. Schmidt, Influence of plant polymers on the distribution and cultivation of bacteria in the phylum *Acidobacteria*, *Appl. Environ. Microbiol.*, 2011, **77**(2), 586–596.

50 D. Fang, G. Zhao, X. Xu, Q. Zhang, Q. Shen, Z. Fang, L. Huang and F. Ji, Microbial community structures and functions of wastewater treatment systems in plateau and cold regions, *Bioresour. Technol.*, 2018, **249**, 684–693.

51 H. M. Jang, J. H. Ha, J. M. Park, M.-S. Kim and S. G. Sommer, Comprehensive microbial analysis of combined mesophilic anaerobic–thermophilic aerobic process treating high-strength food wastewater, *Water Res.*, 2015, **73**, 291–303.
52 Z. Yan, N. Song, H. Cai, J. H. Tay and H. Jiang, Enhanced degradation of phenanthrene and pyrene in freshwater sediments by combined employment of sediment microbial fuel cell and amorphous ferric hydroxide, *J. Hazard. Mater.*, 2012, **199**, 217–225.
53 H. M. Dionisi, A. C. Layton, G. Harms, I. R. Gregory, K. G. Robinson and G. S. Sayler, Quantification of *Nitrosomonas oligotropha*-like ammonia-oxidizing bacteria and *Nitrospira* spp. from full-scale wastewater treatment plants by competitive PCR, *Appl. Environ. Microbiol.*, 2002, **68**(1), 245–253.
54 A. B. Caracciolo, P. Grenni, R. Ciccoli, G. Di Landa and C. Cremisini, Simazine biodegradation in soil: analysis of bacterial community structure by in situ hybridization, *Pest Manage. Sci.*, 2005, **61**(9), 863–869.
55 J. Boonnorat, S. Techkarnjanaruk, R. Honda and P. Prachanurak, Effects of hydraulic retention time and carbon to nitrogen ratio on micro-pollutant biodegradation in membrane bioreactor for leachate treatment, *Bioresour. Technol.*, 2016, **219**, 53–63.
56 N. M. Henderson and R. K. Sutherland, *Nocardia* and *Actinomyces*, *Medicine*, 2017, **45**(12), 753–756.
57 J. Ishikawa, A. Yamashita, Y. Mikami, Y. Hoshino, H. Kurita, K. Hotta, T. Shiba and M. Hattori, The complete genomic sequence of *Nocardia farcinica* IFM 10152, *Proc. Natl. Acad. Sci. U. S. A.*, 2004, **101**, 14925–14930.
58 R. Yang, G. Liu, T. Chen, S. Li, L. An, G. Zhang, G. Li, S. Chang, W. Zhang, X. Chen, X. Wu and B. Zhang, Characterization of the genome of a *Nocardia* strain isolated from soils in the Qinghai-Tibetan Plateau that specifically degrades crude oil and of this biodegradation, *Genomics*, 2018, DOI: 10.1016/j.ygeno.2018.02.010.
59 J. H. Chang, S. K. Rhee, Y. K. Chang and H. N. Chang, Desulfurization of diesel oils by a newly isolated dibenzothiophene-degrading *Nocardia* sp. strain CYKS2, *Biotechnol. Prog.*, 1998, **14**, 851–855.
60 M. Zeinali, M. Vossoughi, S. K. Ardestani, E. Babanezhad and M. Masoumian, Hydrocarbon degradation by thermophilic *Nocardia otitidiscaviarum* strain TSH1: physiological aspects, *J. Basic Microbiol.*, 2007, **47**, 534–539.
61 G. Porcheron and C. M. Dozois, Interplay between iron homeostasis and virulence: Fur and RyhB as major regulators of bacterial pathogenicity, *Vet. Microbiol.*, 2015, **179**(1), 2–14.
62 K. N. Raymond, E. A. Dertz and S. S. Kim, *Enterobactin*: An archetype for microbial iron transport, *Proc. Natl. Acad. Sci. U. S. A.*, 2003, **100**(7), 3584–3588.
63 A. Sikora, J. Wojtowicz-Sienko, P. Piela, U. Zielenkiewicz, K. Tomczyk-Zak, A. Chojnacka, R. Sikora, P. Kowalczyk, E. Grzesiuk and M. Blaszczyk, Selection of bacteria capable of dissimilatory reduction of Fe(III) from a long-term continuous culture on molasses and their use in a microbial fuel cell, *J. Microbiol. Biotechnol.*, 2011, **21**(3), 305–316.
64 N. Haleyur, E. Shahsavari, M. Taha, L. S. Khudur, E. Koshlaf, A. M. Osborn and A. S. Ball, Assessing the degradation efficacy of native PAH-degrading bacteria from aged, weathered soils in an Australian former gasworks site, *Geoderma*, 2018, **321**, 110–117.
65 M. F. Fillat, The FUR (ferric uptake regulator) superfamily: Diversity and versatility of key transcriptional regulators, *Arch. Biochem. Biophys.*, 2014, **546**, 41–52.
66 S. C. Andrews, A. K. Robinson and F. Rodriguez-Quinones, Bacterial iron homeostasis, *FEMS Microbiol. Rev.*, 2003, **27**, 215–237.
67 C. A. Francis, A. Y. Obraztsova and B. M. Tebo, Dissimilatory metal reduction by the facultative anaerobe *Pantoea agglomerans* Sp1, *Appl. Environ. Microbiol.*, 2000, **66**, 543–548.
68 M. M. Abboud, K. M. Khleifat, M. Batarseh, K. A. Tarawneh, A. Al-Mustafa and M. Al-Madadhah, Different optimization conditions required for enhancing the biodegradation of linear alkylbenzosulfonate and sodium dodecyl sulfate surfactants by novel consortium of *Acinetobacter calcoaceticus* and *Pantoea agglomerans*, *Enzyme Microb. Technol.*, 2007, **41**(4), 432–439.
69 J. Schäfer, U. Jäckel and P. Kämpfer, Analysis of *Actinobacteria* from mould-colonized water damaged building material, *Syst. Appl. Microbiol.*, 2010, **33**(5), 260–268.
70 S. Kim and F. W. Picardal, Enhanced anaerobic biotransformation of carbon tetrachloride in the presence of reduced iron oxides, *Environ. Toxicol. Chem.*, 1999, **18**(10), 2142–2150.
71 V. Braun and K. Hantke, Recent insights into iron import by bacteria, *Curr. Opin. Chem. Biol.*, 2011, **15**(2), 328–334.
72 R. Karlin and S. Levi, Diagenesis of magnetic minerals in recent haemipelagic sediments, *Nature*, 1983, **303**, 327.
73 K. A. Weber, L. A. Achenbach and J. D. Coates, Microorganisms pumping iron: anaerobic microbial iron oxidation and reduction, *Nat. Rev. Microbiol.*, 2006, **4**, 752.
74 R. Sekar, H. D. Shin and T. J. DiChristina, Direct conversion of cellulose and hemicellulose to fermentable sugars by a microbially-driven Fenton reaction, *Bioresour. Technol.*, 2016, **218**, 1133–1139.
75 C. J. Lentini, S. D. Wankel and C. M. Hansel, Enriched iron(III)-reducing bacterial communities are shaped by carbon substrate and iron oxide mineralogy, *Front. Microbiol.*, 2012, **3**, 1–14.
76 D. R. Lovley and E. J. P. Phillips, Organic matter mineralization with reduction of ferric Iron in anaerobic sediments, *Appl. Environ. Microbiol.*, 1986, **51**(4), 683.
77 J. E. Kostka and K. H. Nealson, Dissolution and reduction of magnetite by bacteria, *Environ. Sci. Technol.*, 1995, **29**(10), 2535–2540.
78 W. Zhang, X. M. Li, T. X. Liu and F. B. Li, Enhanced nitrate reduction and current generation by *Bacillus* sp. in the presence of iron oxides, *J. Soils Sediments*, 2012, **12**, 354–365.
79 K. P. Nevin and D. R. Lovley, Potential for nonenzymatic reduction of Fe(III) via electron shuttling in subsurface sediments, *Environ. Sci. Technol.*, 2000, **34**, 2472–2478.

